

MAR 19 1969

USA  
F. H. E.

NASA

NATIONAL AERONAUTICS AND SPACE ADMINISTRATION

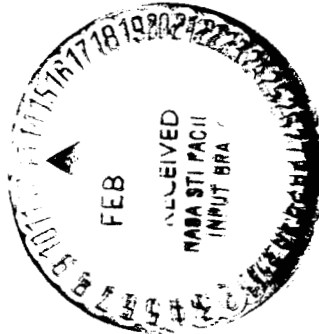
MSC INTERNAL NOTE NO. 69-FM- 62

March 11, 1969

FEB 9 1970

Technical Library, Bellcomm, Inc.

LINEARIZED IMPULSIVE  
EARTH APPROACH  
GUIDANCE ANALYSIS



Advanced Mission Design Branch

MISSION PLANNING AND ANALYSIS DIVISION

MANNED SPACECRAFT CENTER  
HOUSTON, TEXAS



(NASA-TM-X-69711) LINEARIZED IMPULSIVE  
EARTH APPROACH GUIDANCE ANALYSIS (NASA)  
30 p

N74-70854

00/99 Unclass  
16220

MSC INTERNAL NOTE NO. 69-FM-62

---

LINEARIZED IMPULSIVE EARTH APPROACH  
GUIDANCE ANALYSIS

By Thomas B. Murtagh  
Advanced Mission Design Branch

---

March 11, 1969

MISSION PLANNING AND ANALYSIS DIVISION  
NATIONAL AERONAUTICS AND SPACE ADMINISTRATION  
MANNED SPACECRAFT CENTER  
HOUSTON, TEXAS

Approved: 

Jack Funk, Chief  
Advanced Mission Design Branch

Approved: 

John P. Mayer, Chief  
Mission Planning and Analysis Division

## CONTENTS

Section	Page
SUMMARY . . . . .	1
INTRODUCTION . . . . .	1
SYMBOLS . . . . .	2
ANALYSIS . . . . .	4
Initial and Final State Vector Error Relationship . . . . .	4
Generalized Equation for the Velocity Correction . . . . .	5
Fixed Time-of-Arrival Guidance Laws . . . . .	5
Variable Time-of-Arrival Guidance Laws . . . . .	7
Error Propagation for VTA Guidance . . . . .	9
RESULTS AND DISCUSSION . . . . .	11
Reference Trajectory and Assumptions . . . . .	11
Navigation Results . . . . .	12
FTA Guidance Results . . . . .	12
VTA Guidance Results . . . . .	13
CONCLUDING REMARKS . . . . .	14
REFERENCES . . . . .	26

## FIGURES

Figure		Page
1	SOI midcourse $\Delta V$ as a function of entry parameters	
	(a) $i_E = 75^\circ$ , $h_E = 400\ 000\ \text{ft}$ . . . . .	15
	(b) $i_E = 35^\circ$ , $h_E = 400\ 000\ \text{ft}$ . . . . .	16
2	Entry parameter navigation data	
	(a) Radius uncertainty . . . . .	17
	(b) Speed uncertainty . . . . .	18
	(c) Flight-path angle (FPA) uncertainty . . . . .	19
3	Fixed time of arrival guidance data for Earth-entry corridor control	
	(a) Null position vector errors . . . . .	20
	(b) Null radial, cross-range, and flight-path angle (FPA) errors . . . . .	21
4	Variable time of arrival guidance data for Earth-entry corridor control	
	(a) Null position vector errors; minimize the magnitude of the commanded correction . . . . .	22
	(b) Null radial, cross-range, and flight-path angle (FPS) errors; minimize the magnitude of the commanded correction . . . . .	23
	(c) Null radial, cross-range, and flight-path angle (FPS) errors; minimize the distance to the nominal entry point . . . . .	24
	(d) Null position vector errors; choose time variation such that flight-path angle (FPA) errors are zero . . . . .	25

# LINEARIZED IMPULSIVE EARTH APPROACH GUIDANCE ANALYSIS

By Thomas B. Murtagh

## SUMMARY

A comparative analysis is presented of a variety of guidance laws for Earth-entry corridor control on the return leg of a conjunction-class Mars mission. The fixed and variable time-of-arrival guidance laws used for the analysis are derived in a general form. Particular solutions are generated by specification of the constraint equations for the state variables. For the variable time-of-arrival guidance laws, a generalized equation is developed which provides for the propagation of the position and velocity dispersions to the nominal time of arrival at the target. The development includes a calculation of the timing error predicted by the guidance equations. For the type of Earth entry problems considered, results of the analysis indicate that the best overall performance is produced by a variable time-of-arrival guidance law which constrains radial, cross-range, and flight-path angle errors while it minimizes the magnitude of the commanded velocity correction.

## INTRODUCTION

The linear theory of impulsive velocity corrections for space vehicle guidance has been discussed in references 1 through 5. However, the guidance theory contained in these references is restricted to a discussion of fixed and variable time-of-arrival position guidance and no attempt is made to generalize the formulation of the guidance laws. A similarity of form between these guidance laws is evident, which suggests that they are somehow mathematically related. Cicolani (ref. 6) noted this similarity and attempted to determine the general properties of linearized impulsive guidance laws by use of the concepts of linear vector spaces and the pseudoinverse of a matrix. A more straightforward approach to the problem was made by Tempelman (ref. 7) who began with a generalized linear constraint equation and developed a solution to the impulsive guidance problem.

The analysis presented in this document was motivated by Tempelman's work and is an attempt to simplify his approach to the development of a general formulation of linearized impulsive guidance laws. An extension of Tempelman's development is the derivation of a generalized equation for the variable time-of-arrival guidance laws which provides for the propagation of position and velocity dispersions to the nominal time of arrival at the target. A calculation of the timing error predicted by the guidance equations is also included. A comparison of a variety of guidance laws for the Earth entry phase of a conjunction-class Mars mission is presented to illustrate the theory outlined in the preceding paragraph.

## SYMBOLS

$\bar{a}$	acceleration vector
D	distance from nominal target point defined by equation (23)
E	6 by 6 uncertainty covariance matrix defined by equation (43)
$\bar{e}$	uncertainty in state vector estimate
G	6 by 6 guidance-law matrix defined by equation (9)
$G_1, G_2$	3 by 3 submatrices of G
H	3 by 3 guidance-constraint matrix used in equation (6)
$\bar{h}$	orbital angular momentum vector, $\bar{h} = \bar{R} \times \bar{V}$
I	identity matrix of appropriate dimensions
K	3 by 3 guidance-constraint matrix used in equation (6)
$\bar{L}$	guidance-constraint vector used in equation (6)
M	6 by 3 compatibility matrix defined by equation (45)
N	3 by 3 covariance matrix of velocity correction execution error defined by equation (42)
$^*P$	6 by 6 dispersion covariance matrix defined by equation (50)
P	6 by 6 dispersion covariance matrix defined by equation (38)

$R$	magnitude of $\bar{R}$
$\bar{R}$	position vector
$t$	current time
$T$	time of arrival at target point
$V$	magnitude of $\bar{V}$
$\bar{V}$	velocity vector
$\bar{X}$	state vector, $\bar{X} = \begin{bmatrix} \bar{R} \\ \bar{V} \end{bmatrix}$
$\bar{Z}_1$	sensitivity vector that relates flight-path angle error to position vector errors
$\bar{Z}_2$	sensitivity vector that relates flight-path angle error to velocity vector errors
$\bar{\alpha}_1, \bar{\alpha}_2$	timing error sensitivity to position vector errors
$\bar{\beta}_1, \bar{\beta}_2$	timing error sensitivity to velocity vector errors
$\Gamma$	6 by 6 transition matrix defined by equation (36)
$\gamma$	flight-path angle
$\delta( )$	small variation of ( )
$\Delta V$	magnitude of $\Delta \bar{V}$
$\Delta \bar{V}$	velocity correction vector defined by equation (5)
$\bar{n}$	vector defined by equation (15)
$\Phi$	6 by 6 state transition matrix defined by equation (3)
$\phi_1, \phi_2, \phi_3, \phi_4$	3 by 3 submatrices of $\Phi$
$\Phi'$	6 by 6 transition matrix defined by equation (37)
$\Theta$	6 by 6 matrix defined by equation (48)

$\tau$  arbitrary time

$\bar{\xi}$  velocity correction implementation error vector

Superscripts:

$+$  ( ) after maneuver or measurement

$-$  ( ) before maneuver or measurement

$T$  transpose of ( )

$-1$  inverse of ( )

$\langle ( ) \rangle$  expected value of ( )

### ANALYSIS

#### Initial and Final State Vector Error Relationship

The terminal state vector error  $\delta\bar{X}^+(T)$  is related to the initial state vector error  $\delta\bar{X}^+(t)$  through the state transition matrix  $\phi(T, t)$  as

$$\delta\bar{X}^+(T) = \phi(T, t)\delta\bar{X}^+(t) + \begin{bmatrix} \bar{V}(T) \\ \bar{a}(T) \end{bmatrix} \delta T \quad (1)$$

where  $\bar{V}(T)$  and  $\bar{a}(T)$  are the velocity and acceleration, respectively, of the nominal trajectory at the nominal time of arrival at the target  $T$ . If  $\delta\bar{X}(\tau)$  is defined by

$$\delta\bar{X}(\tau) = \begin{bmatrix} \delta\bar{R}(\tau) \\ \delta\bar{V}(\tau) \end{bmatrix} \quad (2)$$

where  $\tau$  is some arbitrary time and if the state transition matrix  $\phi(T, t)$  is partitioned into

$$\phi(T, t) = \begin{bmatrix} \phi_1(T, t) & \phi_2(T, t) \\ \phi_3(T, t) & \phi_4(T, t) \end{bmatrix} \quad (3)$$

then equation (1) can be written (ref. 7)

$$\delta\bar{R}^+(T) = \phi_1\delta\bar{R}^+(t) + \phi_2\delta\bar{V}^+(t) + \bar{V}(T)\delta T \quad (4a)$$

$$\bar{V}^+(T) = \phi_3\delta\bar{R}^+(t) + \phi_4\delta\bar{V}^+(t) + \bar{a}(T)\delta T \quad (4b)$$

where the timescripts on the transition matrix have been omitted for notational simplicity.



## Generalized Equation for the Velocity Correction

The velocity correction  $\Delta \bar{V}(t)$  is defined by

$$\Delta \bar{V}(t) = \delta \bar{V}^+(t) - \delta \bar{V}^-(t) \quad (5)$$

If terminal constraints consistent with the guidance law being investigated are imposed and if those constraint relationships are substituted into equation (4), an equation results in the form

$$\delta \bar{V}^+(t) = -K^{-1}H\delta \bar{R}^+(t) - K^{-1}\bar{L}\delta T \quad (6)$$

where  $K$  and  $H$  are guidance constraint matrices and where  $\bar{L}$  is a guidance constraint vector. By use of the fact that if the maneuver is assumed to be impulsive, that is,

$$\delta \bar{R}^+(t) = \delta \bar{R}^-(t) \quad (7)$$

and if equations (5), (6), and (7) are combined with the expression for  $\delta T$  as a function of position and velocity deviations at the time of the correction, a general form of the equation for the velocity correction is derived as

$$\Delta \bar{V}(t) = G_1 \delta \bar{R}^-(t) + G_2 \delta \bar{V}^-(t) \quad (8)$$

where  $G_1$  and  $G_2$  are submatrices of the guidance law matrix (refs. 4 and 6).

$$G = \begin{bmatrix} 0 & 0 \\ G_1 & G_2 \end{bmatrix} \quad (9)$$

## Fixed Time-of-Arrival Guidance Laws

For fixed time-of-arrival (FTA) guidance laws  $\delta T = 0$  and equation (6) becomes

$$\delta \bar{V}^+(t) = -K^{-1}H\delta \bar{R}^-(t) \quad (10)$$

The most commonly used FTA guidance law imposes the constraint that

$$\delta \bar{R}^+(T) = 0 \quad (11)$$

and is referred to as FTA position guidance (refs. 1 through 4). Use of equations (7) and (11) with equation (4a) produces the expression

$$\delta \bar{V}^+(t) = -\phi_2^{-1}\phi_1 \bar{R}^-(t) \quad (12)$$

A comparison of equations (10) and (12) indicates that for this guidance law  $K = \phi_2$  and  $H = \phi_1$ . Use of equations (5) and (12) and

comparison of the resultant expression with equation (8) produces

$$\left. \begin{aligned} G_1 &= -\phi_2^{-1} \phi_1 \\ G_2 &= -I \end{aligned} \right\} \quad (13)$$

for an FTA position guidance law where  $I$  is the identity matrix. Another type of FTA guidance law might seek to constrain the radial, cross-range, and flight-path angle errors at some terminal time  $T$ . The radial error is defined as the component of the position error along the radius vector; the cross-range error is defined as the component of the position error along the orbital angular momentum vector. The resultant constraint equations are

$$\left. \begin{aligned} \bar{\eta}^T \delta \bar{V}^+(T) - \bar{V}^T \delta \bar{R}^+(T) &= 0 \\ \bar{R}^T \delta \bar{R}^+(T) &= 0 \\ \bar{h}^T \delta \bar{R}^+(T) &= 0 \end{aligned} \right\} \quad (14)$$

where  $\bar{h}$  is a vector in the direction of the orbital angular momentum and where

$$\bar{h} = \frac{(\bar{R} \times \bar{V}) \times \bar{V}}{v^2} \quad (15)$$

If the constraint equation (14) is combined with equation (4), the following expressions are produced for the matrices  $K$  and  $H$  in equation (10).

$$K = \begin{bmatrix} (\bar{\eta}^T \phi_4 - \bar{V}^T \phi_2) \\ \bar{R}^T \phi_2 \\ \bar{h}^T \phi_2 \end{bmatrix} \quad (16a)$$

$$H = \begin{bmatrix} (\bar{\eta}^T \phi_3 - \bar{V}^T \phi_1) \\ \bar{R}^T \phi_1 \\ \bar{h}^T \phi_1 \end{bmatrix} \quad (16b)$$

The matrices  $G_1$  and  $G_2$  are shown to be

$$\left. \begin{aligned} G_1 &= -K^{-1}H \\ G_2 &= -I \end{aligned} \right\} \quad (17)$$

Other types of FTA guidance laws can be generated if the appropriate constraints are imposed and if the final expression is in the form of

equation (8). Stern (ref. 2) develops FTA guidance laws which are derived by the imposition of constraints on certain combinations of the Keplerian orbital elements.

### Variable Time-of-Arrival Guidance Laws

The most popular variable time-of-arrival (VTA) guidance law is the VTA position guidance law which requires that  $\delta \bar{R}^+(T) = 0$  and which computes  $\delta T$  ( $\delta T \neq 0$  for any VTA guidance law) to minimize the magnitude of the commanded velocity correction  $\Delta \bar{V}(t)$ . For this guidance law, the matrices  $K$  and  $H$  in equation (6) are equal to  $\phi_2$  and  $\phi_1$ , respectively, and the vector  $\bar{L}$  is equal to  $\bar{V}(T)$  (refs. 1 through 4).

A similar VTA guidance law is generated if the constraints in equations (14) (i.e., null radial, cross-range, and flight-path angle errors) are imposed to produce the expressions for the matrices  $K$  and  $H$  in equation (16) and the following equation for the vector  $\bar{L}$  required for the general equation (6).

$$\bar{L} = \begin{bmatrix} (\bar{n}^T \bar{a} - \bar{V}^T \bar{V}) \\ \bar{R}^T \bar{V} \\ 0 \end{bmatrix} \quad (18)$$

where  $\bar{n}$  is defined in equation (15). Combination of equations (5), (6), and (7) results in

$$\Delta \bar{V}(t) = -K^{-1} H \delta \bar{R}^-(t) - \delta \bar{V}^-(t) - K^{-1} \bar{L} \delta T \quad (19)$$

The next step is to compute  $\delta T$  so as to minimize the magnitude of the commanded velocity correction. This computation requires the solution of the following expression for  $\delta T$ .

$$\Delta \bar{V}^T(t) \frac{\partial \Delta \bar{V}(t)}{\partial (\delta T)} = 0 \quad (20)$$

Use of equations (19) and (20) yields

$$\delta T = - \frac{(K^{-1} \bar{L})^T K^{-1} H \delta \bar{R}^-(t) + (K^{-1} \bar{L})^T \delta \bar{V}^-(t)}{(K^{-1} \bar{L})^T (K^{-1} \bar{L})} \quad (21)$$

Substitution of equation (21) into (19) and comparison of the resultant equation with equation (8) provides expressions for  $G_1$  and  $G_2$ .

$$\left. \begin{aligned} G_1 &= G_2 K^{-1} H \\ G_2 &= \frac{(K^{-1} \bar{L})(K^{-1} \bar{L})^T}{(K^{-1} \bar{L})^T (K^{-1} \bar{L})} - I \end{aligned} \right\} \quad (22)$$

The constraints on radial, cross-range, and flight-path angle errors represented by equations (14) may also be used to construct a VTA guidance law which computes  $\delta T$  to minimize the distance from the nominal target point  $D$ . This distance is given by the expression

$$D = [\delta \bar{R}^+(T)]^T \delta \bar{R}^+(T) \quad (23)$$

where  $\delta \bar{R}^+(T)$  is defined by equation (4a) (ref. 7). The equation

$$[\delta \bar{R}^+(T)]^T \frac{\partial \delta \bar{R}^+(T)}{\partial (\delta T)} = 0 \quad (24)$$

must be solved in combination with the equation for  $\delta \bar{R}^+(T)$  to produce

$$\delta T = - \frac{(\bar{V} - \phi_2 K^{-1} \bar{L})^T (\phi_1 - \phi_2 K^{-1} H) \delta \bar{R}^-(t)}{(\bar{V} - \phi_2 K^{-1} \bar{L})^T (\bar{V} - \phi_2 K^{-1} \bar{L})} \quad (25)$$

Substitution of equation (25) into equation (19) and comparison of the resultant expression with equation (8) produces the following equations.

$$\left. \begin{aligned} G_1 &= \frac{K^{-1} \bar{L} (\bar{V} - \phi_2 K^{-1} \bar{L})^T (\phi_1 - \phi_2 K^{-1} H)}{(\bar{V} - \phi_2 K^{-1} \bar{L})^T (\bar{V} - \phi_2 K^{-1} \bar{L})} - K^{-1} H \\ G_2 &= -I \end{aligned} \right\} \quad (26)$$

The last type of VTA guidance law to be considered is one which requires that  $\delta \bar{R}^+(T) = 0$  and which computes  $\delta T$  such that the variation in flight-path angle at the target after the correction is zero. The relationship between the flight-path angle variation  $\delta \gamma^+(T)$  and the variations in position and velocity is given by equation (27) (ref. 4).

$$\delta \gamma^+(T) = \bar{Z}_1^T \delta \bar{R}^+(T) + \bar{Z}_2^T \delta \bar{V}^+(T) \quad (27)$$

where

$$\bar{Z}_1 = \frac{\bar{R} \times (\bar{R} \times \bar{V})}{R^2 |\bar{R} \times \bar{V}|} \quad (28)$$

and where

$$\bar{Z}_2 = \frac{(\bar{R} \times \bar{V}) \times \bar{V}}{V^2 |\bar{R} \times \bar{V}|} \quad (29)$$

The vectors  $\bar{Z}_1$  and  $\bar{Z}_2$  represent the sensitivity of the flight-path angle error to position and velocity errors, respectively. If equation (27) is combined with equation (4b) and if the following constraints are imposed

$$\left. \begin{aligned} \delta \bar{R}^+(T) &= 0 \\ \delta \bar{V}^+(T) &= 0 \end{aligned} \right\} \quad (30)$$

then

$$\delta T = - \frac{\bar{Z}_2^T \phi_3 \delta \bar{R}^-(t) + \bar{Z}_2^T \phi_4 \delta \bar{V}^+(t)}{\bar{Z}_2^T \bar{a}} \quad (31)$$

If equation (31) is substituted into equation (19) [ $K = \phi_2$ ,  $H = \phi_1$  and  $\bar{L} = \bar{V}(T)$ ] and if the result is compared with equation (8), equation (32) results.

$$\left. \begin{aligned} G_1 &= - \left[ (\bar{Z}_2^T \bar{a}) \phi_2 - \bar{V} \bar{Z}_2^T \phi_4 \right]^{-1} \left[ (\bar{Z}_2^T \bar{a}) \phi_1 - \bar{V} \bar{Z}_2^T \phi_3 \right] \\ G_2 &= -I \end{aligned} \right\} \quad (32)$$

#### Error Propagation for VTA Guidance

The equation for the variation in the time of arrival  $\delta T$  may be cast into either of the following forms.

$$\delta T = \bar{\alpha}_1^T \delta \bar{R}^+(t) + \bar{\beta}_1^T \delta \bar{V}^+(t) \quad (33)$$

or

$$\delta T = \bar{\alpha}_2^T \delta \bar{R}^-(t) + \bar{\beta}_2^T \delta \bar{V}^-(t) \quad (34)$$

where  $\bar{\alpha}_1$ ,  $\bar{\alpha}_2$ , and  $\bar{\beta}_1$ ,  $\bar{\beta}_2$  are the sensitivities of the timing error to position and velocity errors, respectively. If the expression for  $\delta T$  is like equation (33), then the equation for propagation of the state vector errors (eq. 1) becomes

$$\delta \bar{X}^+(T) = \Gamma(T, t) \delta \bar{X}^+(t) \quad (35)$$

where

$$\Gamma(T, t) = \Phi(T, t) + \Phi'(T, t) \quad (36)$$

and

$$\Phi'(T, t) = \begin{bmatrix} \bar{V}\bar{\alpha}_1^T & \bar{V}\bar{\beta}_1^T \\ \bar{a}\bar{\alpha}_1^T & \bar{a}\bar{\beta}_1^T \end{bmatrix} \quad (37)$$

The covariance matrix of state vector dispersions is defined by

$$P(\tau) = \langle \delta \bar{X}(\tau) \delta \bar{X}^T(\tau) \rangle \quad (38)$$

where the angular brackets denote the expected value operator. If equation (35) is multiplied on the right by its transpose and the expected value of the result is used with the definition in equation (38), the following equation is produced.

$$P^+(T) = \Gamma(T, t) P^+(t) \Gamma^T(T, t) \quad (39)$$

where (ref. 4)

$$P^+(t) = [I + G][P^-(t) - E^-(t)][I + G]^T + E^+(t) \quad (40)$$

and

$$E^+(t) = E^-(t) + \begin{bmatrix} 0 & 0 \\ 0 & N(t) \end{bmatrix} \quad (41)$$

The matrix  $N(t)$  is the covariance matrix of the velocity correction error (derived and discussed in ref. 3) and is defined by

$$N(t) = \langle \bar{\xi}(t) \bar{\xi}^T(t) \rangle \quad (42)$$

where  $\bar{\xi}(t)$  is the velocity correction implementation error vector. The matrix  $E(t)$  is a measure of the navigation system accuracy (refs. 1, 3, and 8) and is defined by

$$E(\tau) = \langle \bar{e}(\tau) \bar{e}^T(\tau) \rangle \quad (43)$$

where  $\bar{e}(\tau)$  is the uncertainty in the state vector estimate.

If the expression for  $\delta T$  is in the form of equation (34), then the derivation of an equation similar to equation (39) requires more complex mathematical manipulations. It is shown in reference 1 that

$$\delta \bar{X}^+(t) = (I + G) \delta \bar{X}^-(t) + G \bar{e}^-(t) - M \bar{\xi} \quad (44)$$

where

$$M = \begin{bmatrix} 0 \\ I \end{bmatrix} \quad (45)$$

Substitution of equation (34) into equation (1) yields

$$\delta \bar{X}^+(T) = \phi \delta \bar{X}^+(t) + \begin{bmatrix} \bar{V}_{\alpha_2}^T & \bar{V}_{\beta_2}^T \\ \bar{a}_{\alpha_2}^T & \bar{a}_{\beta_2}^T \end{bmatrix} \delta \bar{X}^-(t) \quad (46)$$

and insertion of equation (44) into the above expression produces

$$\delta \bar{X}^+(T) = \Theta(T, t) \delta \bar{X}^-(t) + \phi G \bar{e}^-(t) - \phi M \bar{e}^- \quad (47)$$

where

$$\Theta(T, t) = \phi(I + G) + \phi' \quad (48)$$

If equation (47) is multiplied on the right by its transpose and if the expected value of the result is used and terms are collected equation (49) is produced.

$$\begin{aligned} P^+(T) &= P^{*+}(T) + \phi [(I + G)P^-(t) - GE^-(t)] \phi'^T \\ &+ \phi' [P^-(t)(I + G)^T - E^-(t)G^T] \phi^T \\ &+ \phi' P^-(t) \phi'^T \end{aligned} \quad (49)$$

where

$$P^{*+}(T) = \phi P^+(t) \phi'^T \quad (50)$$

## RESULTS AND DISCUSSION

### Reference Trajectory and Assumptions

The reference trajectory chosen to illustrate the guidance laws developed in the preceding sections was a 1977 Mars stopover mission discussed in considerable detail in reference 8. This mission consists of a 360-day outbound phase, a 300-day parking-orbit phase, and a 320-day return phase. The root-mean-square (RMS) position and velocity errors at the termination of the orbit phase were 2 n. mi. and 5 fps, respectively. The uncertainty covariance matrix  $E(t)$  was updated on the return leg by processing both Earth-based radar and onboard optical

navigation data with a Kalman filter; the dispersion covariance matrix  $P(t)$  was updated with three FTA velocity corrections that required a total  $\Delta V$  of 55 fps.

The maneuver required to target the spacecraft to the entry corridor was assumed to be executed at the Earth sphere of influence (SOI), which is approximately 500 000 n. mi. from the Earth. The nominal entry conditions were arbitrarily chosen to be an entry altitude  $h_E$  of 400 000 feet and an entry flight-path angle (FPA)  $\gamma_E$  of  $-6^\circ$  which resulted in an entry speed  $V_E$  of 38 250 fps. The inclination of the entry trajectory  $i_E$  was  $75^\circ$  with no plane change assumed in the targeting maneuver. The time required for the spacecraft to reach the entry interface from the Earth SOI was 64 hours.

A plot is presented in figure 1(a) of the SOI midcourse  $\Delta V$  as a function of the entry speed and FPA for  $h_E = 400\,000$  feet and  $i_E = 75^\circ$ ; a similar plot is presented in figure 1(b) for  $i_E = 35^\circ$  (a plane change of  $40^\circ$ ). The two curves presented on each of these figures bound the flight-path angle between  $0^\circ$  and  $-45^\circ$ . For the previously specified  $h_E$ ,  $V_E$ , and  $\gamma_E$ , and  $i_E = 75^\circ$  the SOI midcourse  $\Delta V$  was 41 fps; for  $i_E = 35^\circ$ , the  $\Delta V$  was 188 fps.

#### Navigation Results

The RMS entry radius, speed, and FPA uncertainties are presented in figure 2. It was assumed that Earth-based radar range and range-rate navigation data were processed every hour from the time of the SOI midcourse maneuver. The solid curves on the figures represent the uncertainties for  $i_E = 75^\circ$ , while the dashed curves represent data for  $i_E = 35^\circ$ . It is evident from these plots that the radar measurements reduce the uncertainty in the entry parameters to a negligible level after 20 hours of tracking.

#### FTA Guidance Results

The RMS entry radius, speed, and FPA dispersions are presented in figure 3 as a function of the RMS  $\Delta V$  for the two FTA guidance laws considered in this paper. For this data and for the VTA guidance data in the following section, the guidance maneuver execution errors, represented by  $N(t)$  in equation (42), assume a 1 percent proportional



error, a  $1^\circ$  pointing error, and a 0.5 fps engine cutoff error (ref. 4). Earth-based radar measurements were assumed to be made once per hour.

The guidance law attempts to null position vector errors at the nominal time of arrival at the entry interface [fig. 3(a)]. It is evident from the figure that there is an optimum time at which to execute the maneuver in order to produce minimum values of the entry parameter dispersions for the smallest propellant expenditure. However, the optimum time is different for each of the entry parameter dispersion plots. The techniques used in reference 9 could be used to determine analytically the optimum single correction times, but this is beyond the scope of this paper.

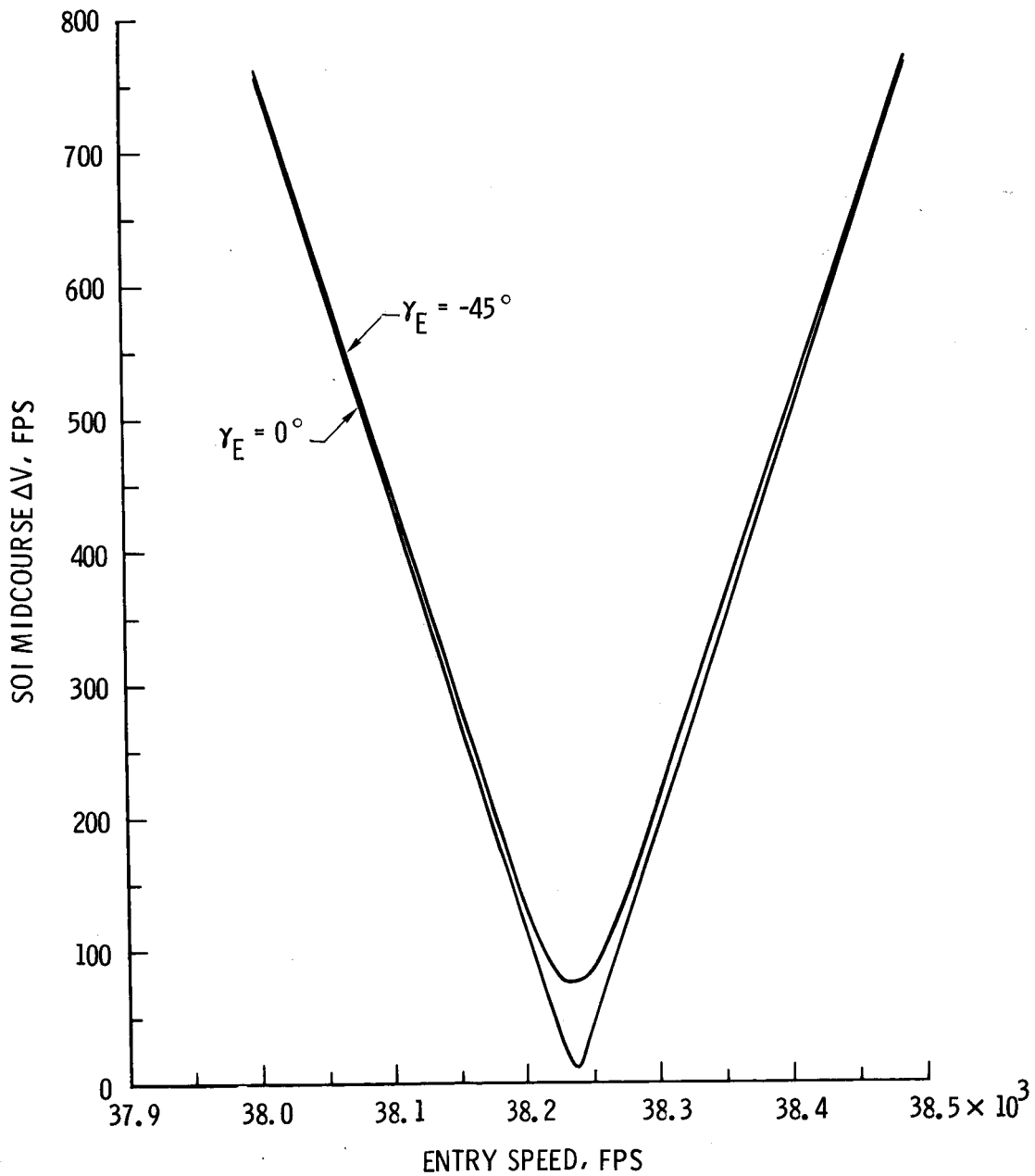
The guidance law attempts to null radial, cross-range, and FPA errors at the nominal time of arrival at the entry interface [fig. 3(b)]. Comparison of the curves in figure 3(b) to those presented in figure 3(a) indicates that the radius and speed errors are approximately equal for either guidance law but that the FPA control is better for the guidance law illustrated in figure 3(b).

#### VTA Guidance Results

The RMS entry radius, speed, and FPA dispersions are presented in figure 4 for the four VTA guidance laws considered. The entry speed errors in figure 4 are generally lower than the corresponding errors presented in figure 3 for the FTA guidance laws. This difference is misleading because for the VTA guidance laws there is an associated plot of the RMS timing error (data not shown) which maps into a velocity error, and this error must be added to the speed error computed from the VTA guidance equations. Typical timing errors for the VTA guidance laws considered range from 150 to 300 seconds. However, the relaxation of the constraint on the time of arrival permits a smaller RMS  $\Delta V$  requirement for specified radius and FPA errors. For example, suppose that an RMS  $\Delta V$  of 25 fps is allowed. In figure 4(a), this  $\Delta V$  is shown to produce a radius error of 0.7 n. mi. and an FPA error of  $0.05^\circ$ ; in figure 4(b), the radius and FPA errors are 0.6 n. mi. and  $0.005^\circ$ , respectively; in figure 4(c), the radius and FPA errors are 3.0 n. mi. and  $0.14^\circ$ , respectively; and in figure 4(d), the resultant radius and FPA errors are 2.2 n. mi. and  $0.01^\circ$ , respectively. These data indicate that the best overall performance is produced by the guidance law which attempts to null radial, cross-range, and FPA errors while it minimizes the magnitude of the commanded correction [fig. 4(b)].

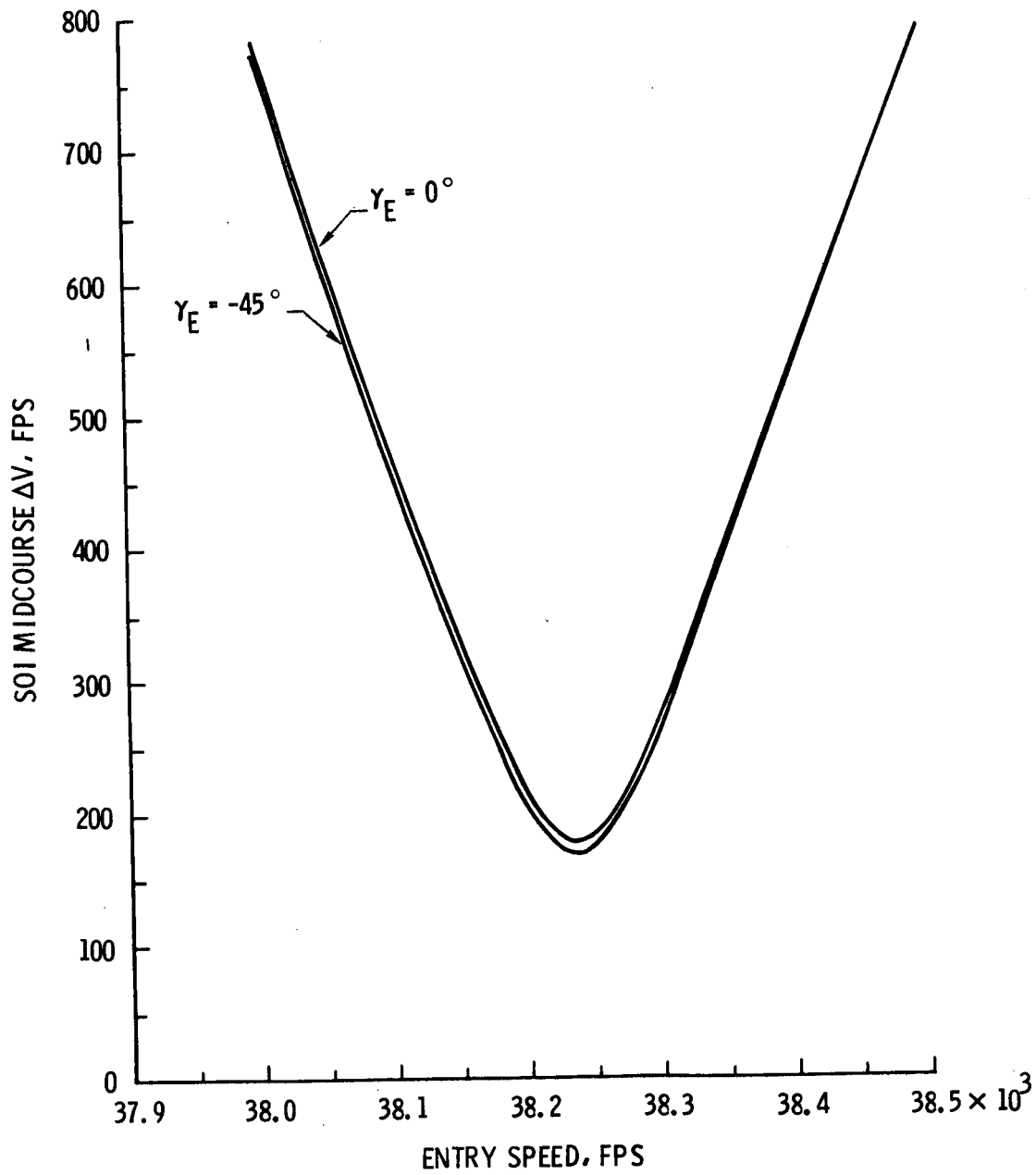
## CONCLUDING REMARKS

A comparative analysis of a variety of guidance laws for the Earth entry phase of a conjunction-class Mars mission has been presented. The fixed and variable time-of-arrival guidance laws used for the analysis were derived in a general form. The results of the analysis indicate that a VTA guidance law which constrains radial, cross-range, and flight-path angle errors while it minimizes the magnitude of the commanded correction produces the most satisfactory performance.



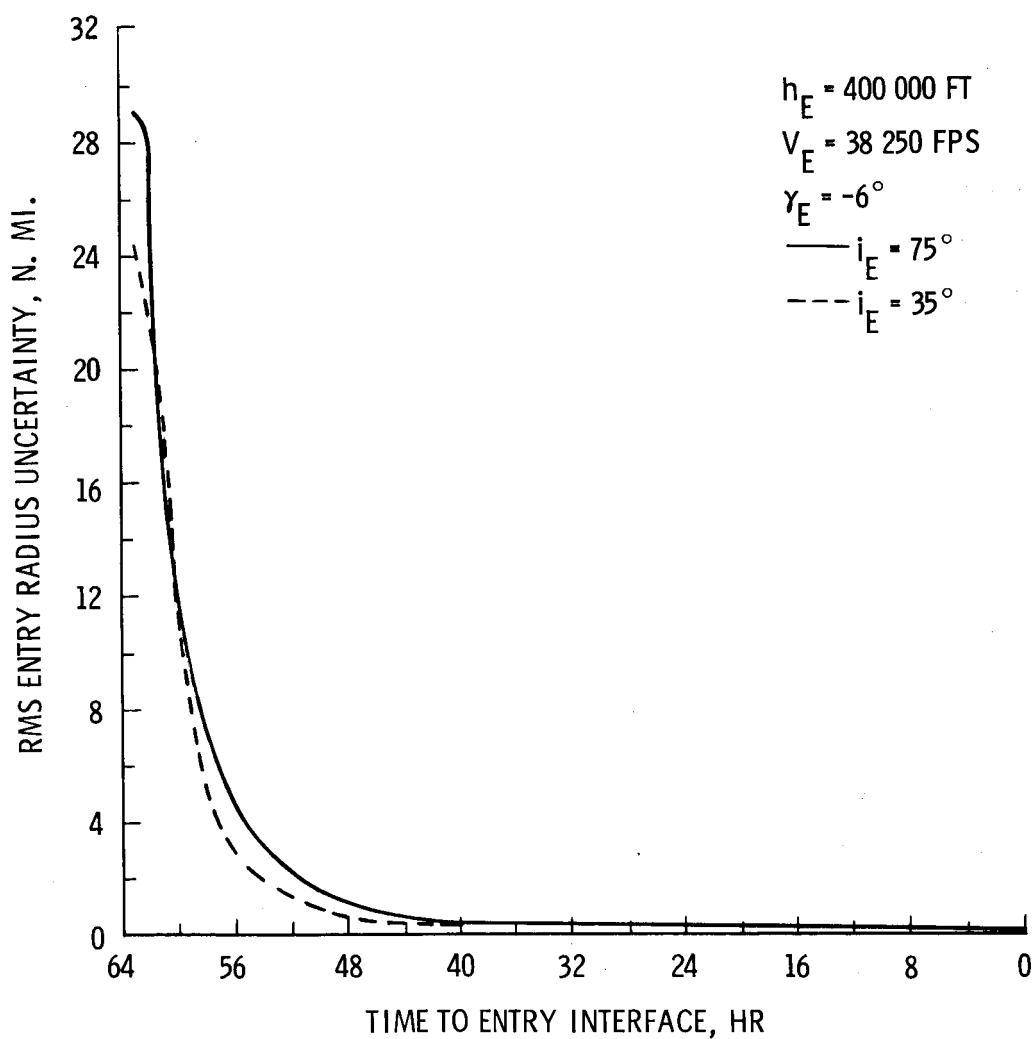
(A)  $i_E = 75^\circ$ ,  $h_E = 400\,000$  FT.

FIGURE 1.- SOI MIDCOURSE  $\Delta V$  AS A FUNCTION OF ENTRY PARAMETERS.



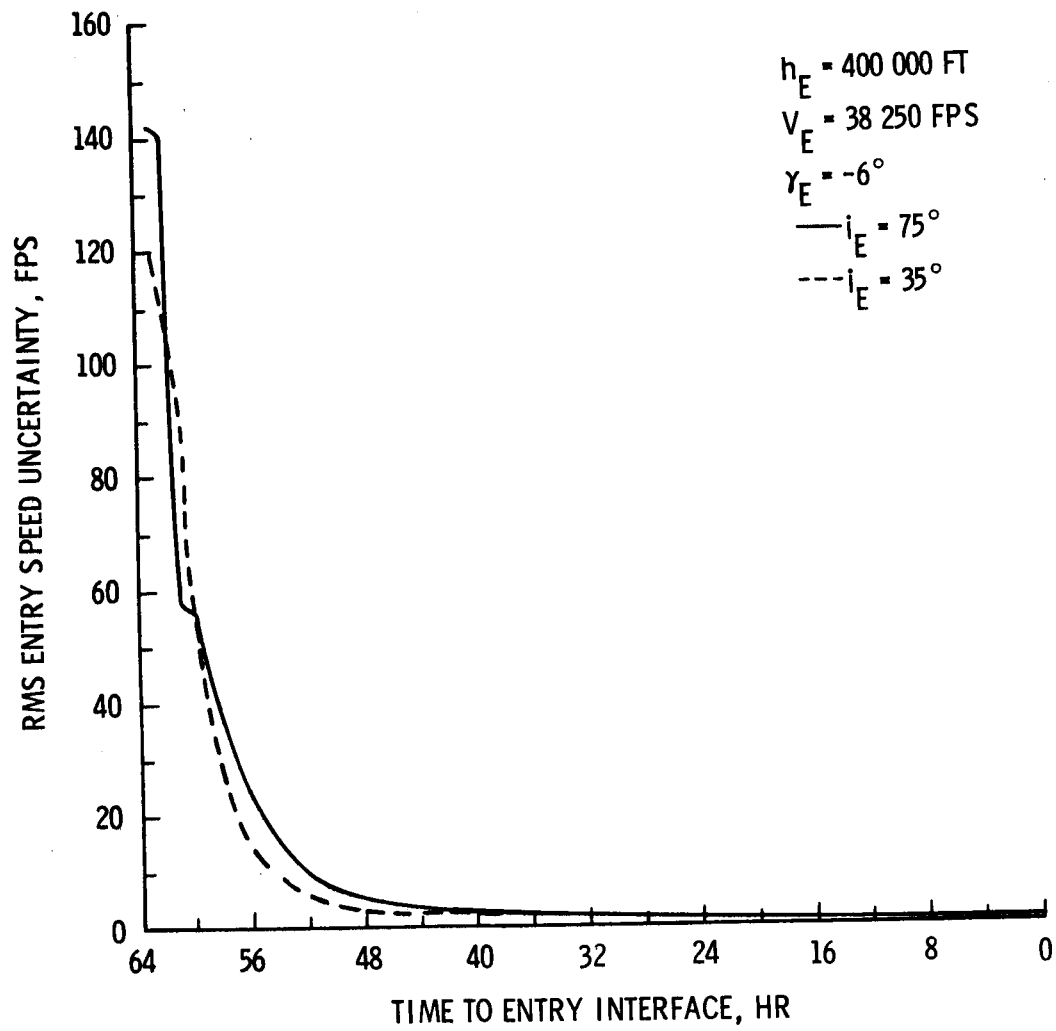
(B)  $i_E = 35^\circ$ ,  $h_E = 400\,000$  FT.

FIGURE 1. - CONCLUDED.



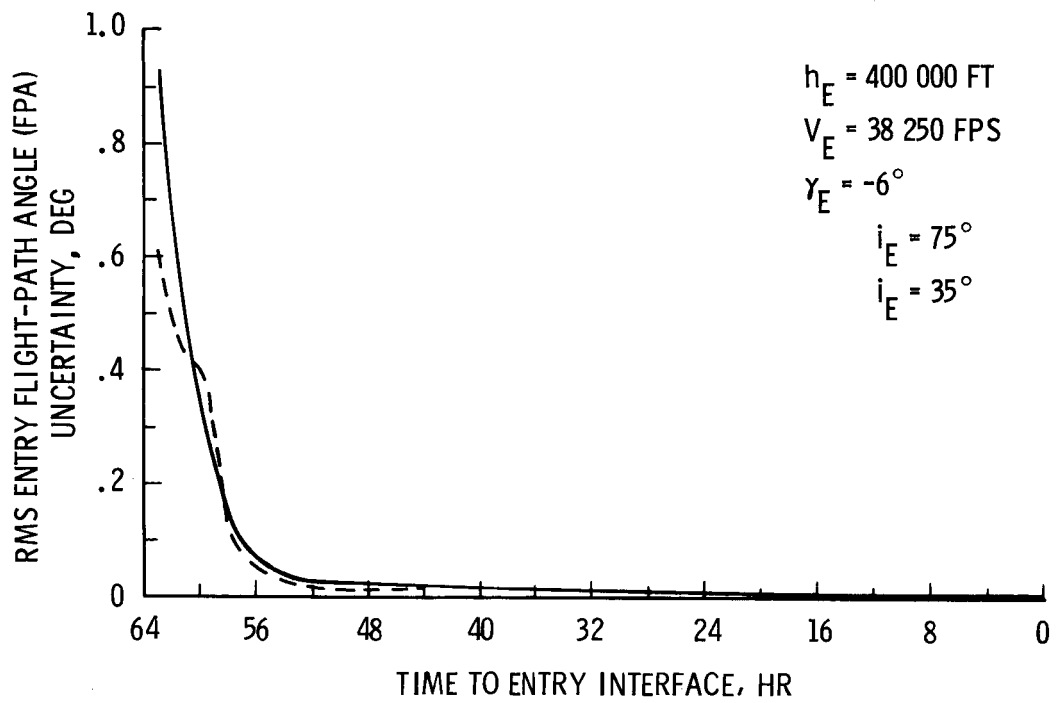
(A) RADIUS UNCERTAINTY.

FIGURE 2. - ENTRY PARAMETER NAVIGATION DATA.



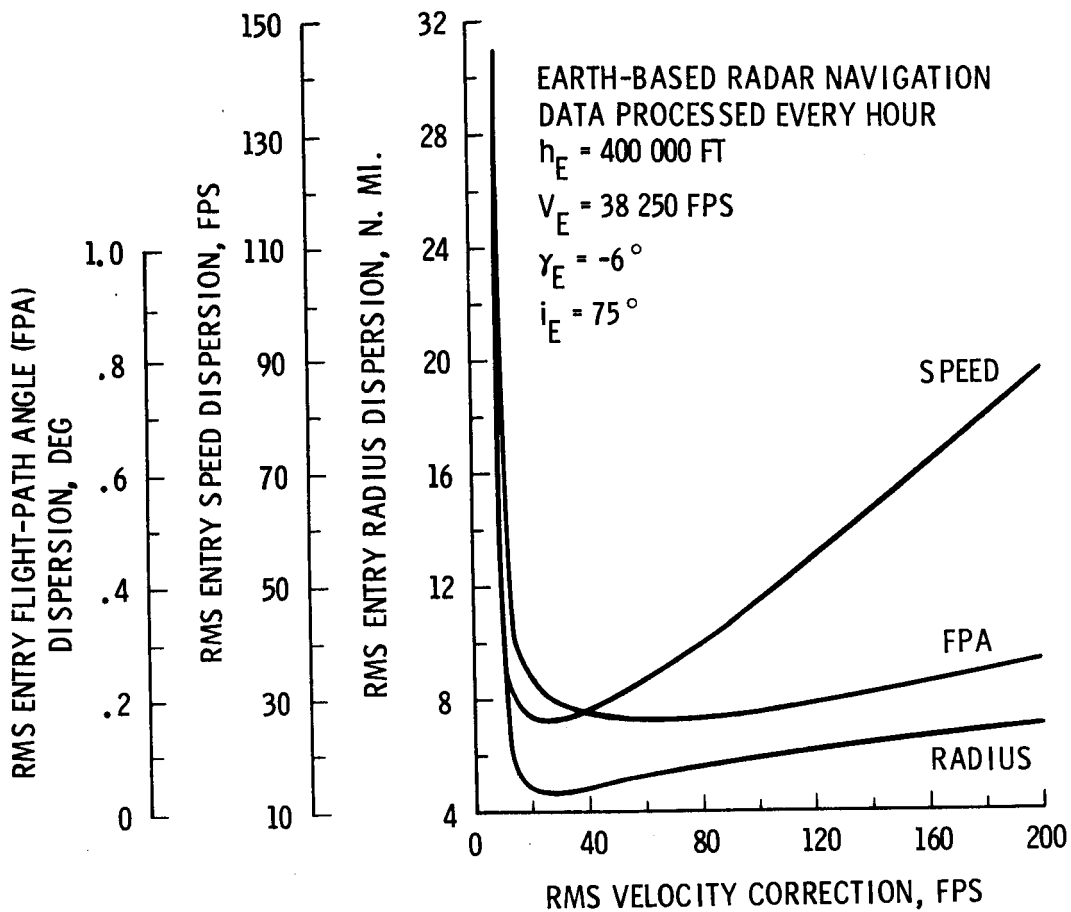
(B) SPEED UNCERTAINTY.

FIGURE 2. - CONTINUED.



(C) FLIGHT-PATH ANGLE (FPA) UNCERTAINTY.

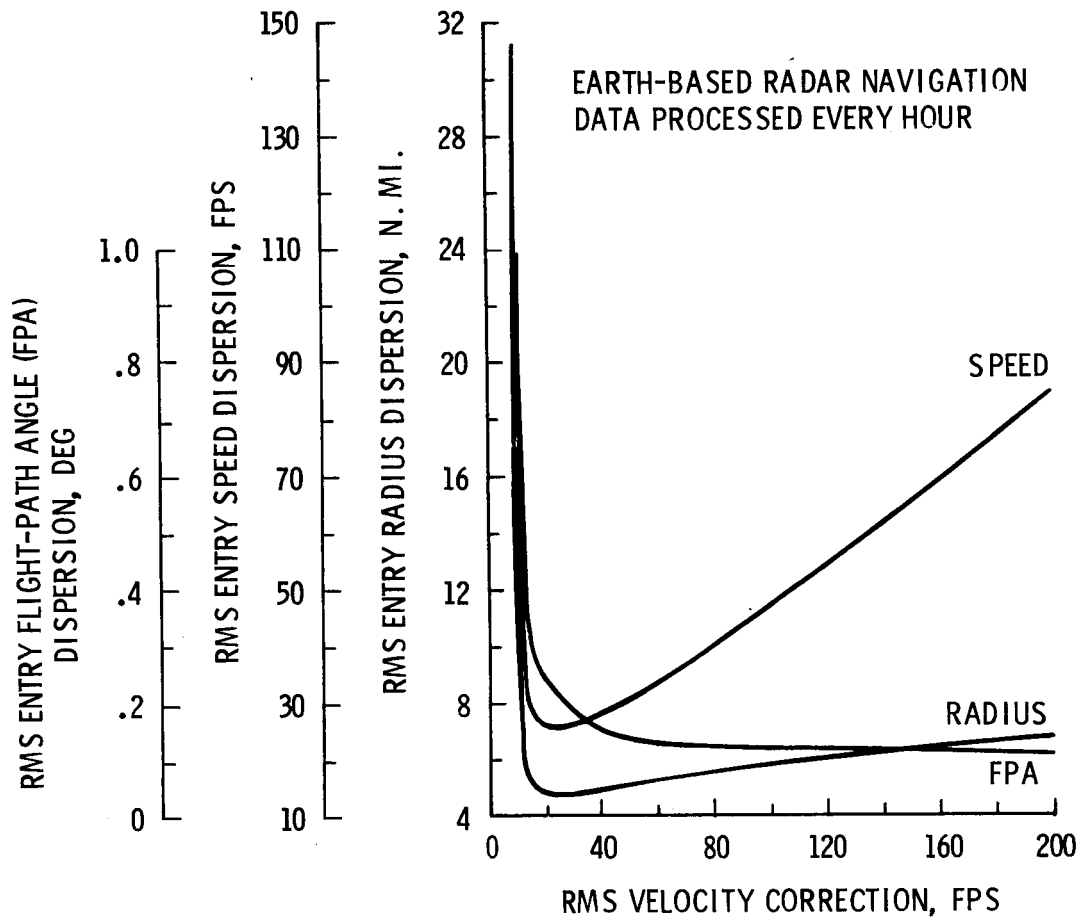
FIGURE 2. - CONCLUDED.



(A) NULL POSITION VECTOR ERRORS.

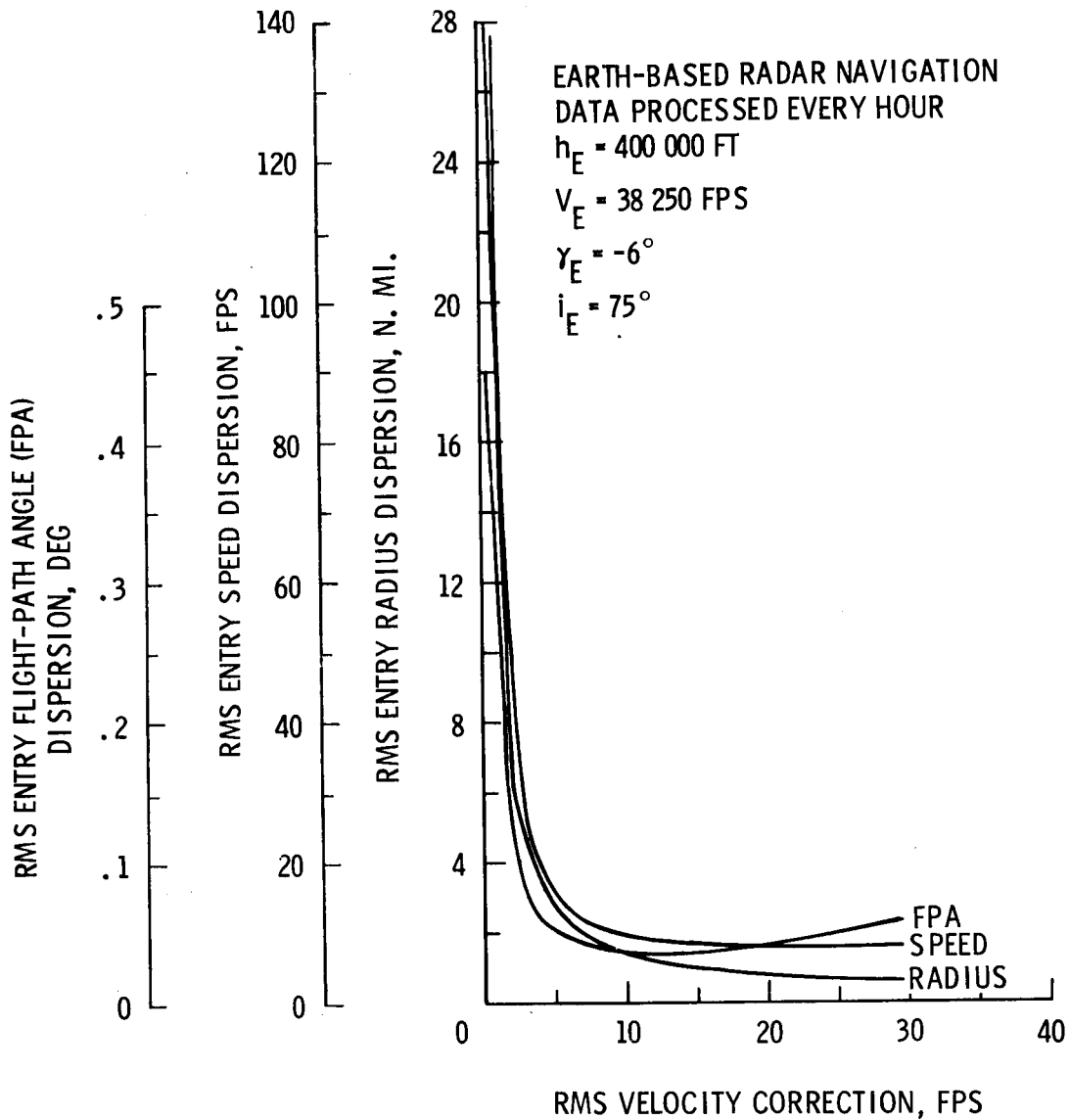
FIGURE 3. - FIXED TIME OF ARRIVAL  
GUIDANCE DATA FOR EARTH-  
ENTRY CORRIDOR CONTROL.





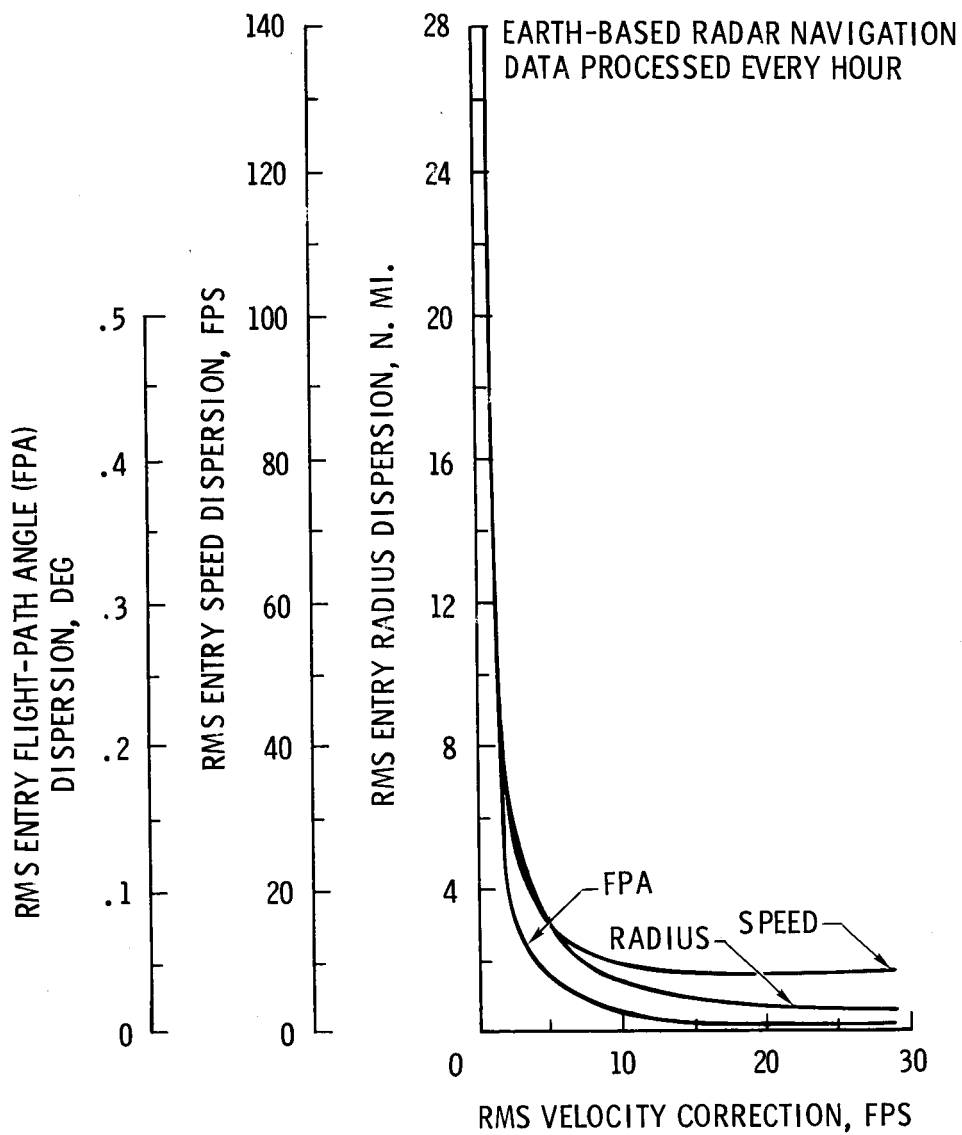
(B) NULL RADIAL, CROSS-RANGE, AND  
FLIGHT-PATH ANGLE (FPA) ERRORS.

FIGURE 3.- CONCLUDED.



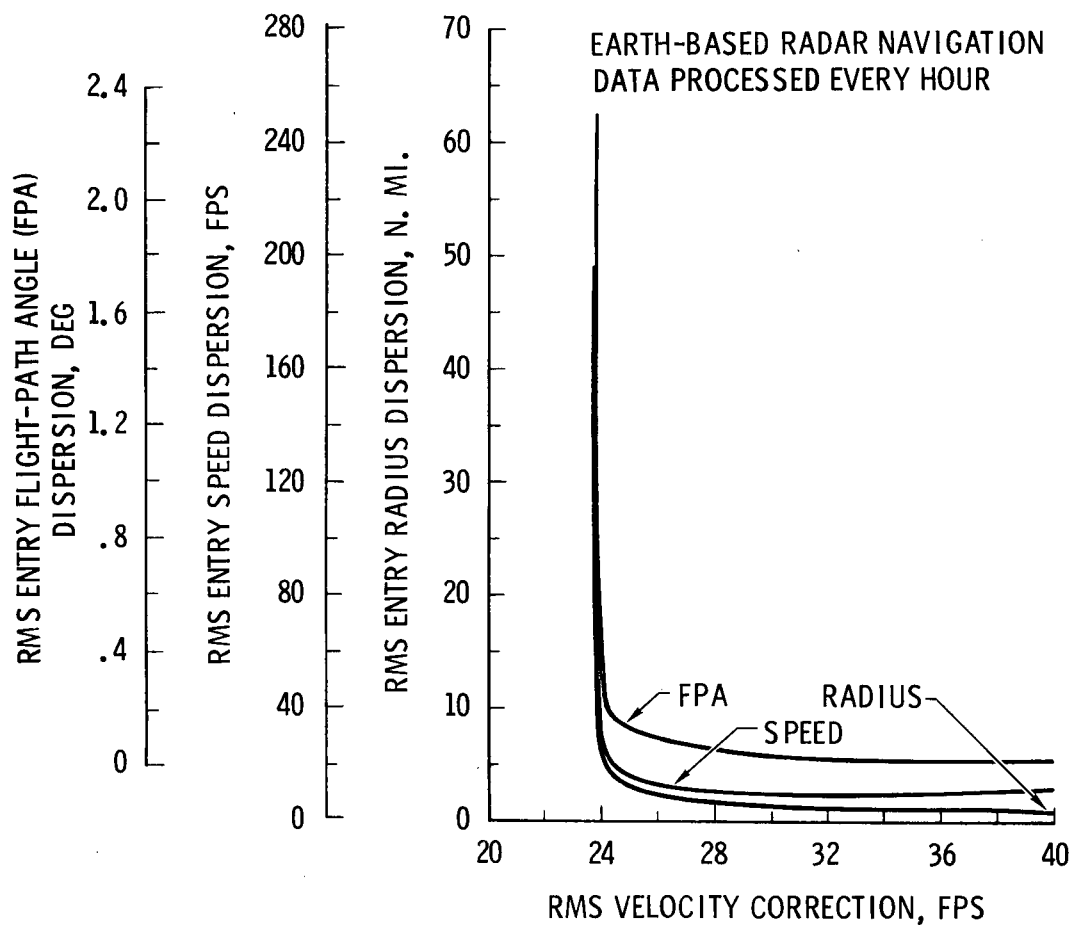
(A) NULL POSITION VECTOR ERRORS;  
MINIMIZE THE MAGNITUDE  
OF THE COMMANDED CORRECTION.

FIGURE 4. - VARIABLE TIME OF ARRIVAL  
GUIDANCE DATA FOR EARTH-ENTRY  
CORRIDOR CONTROL.



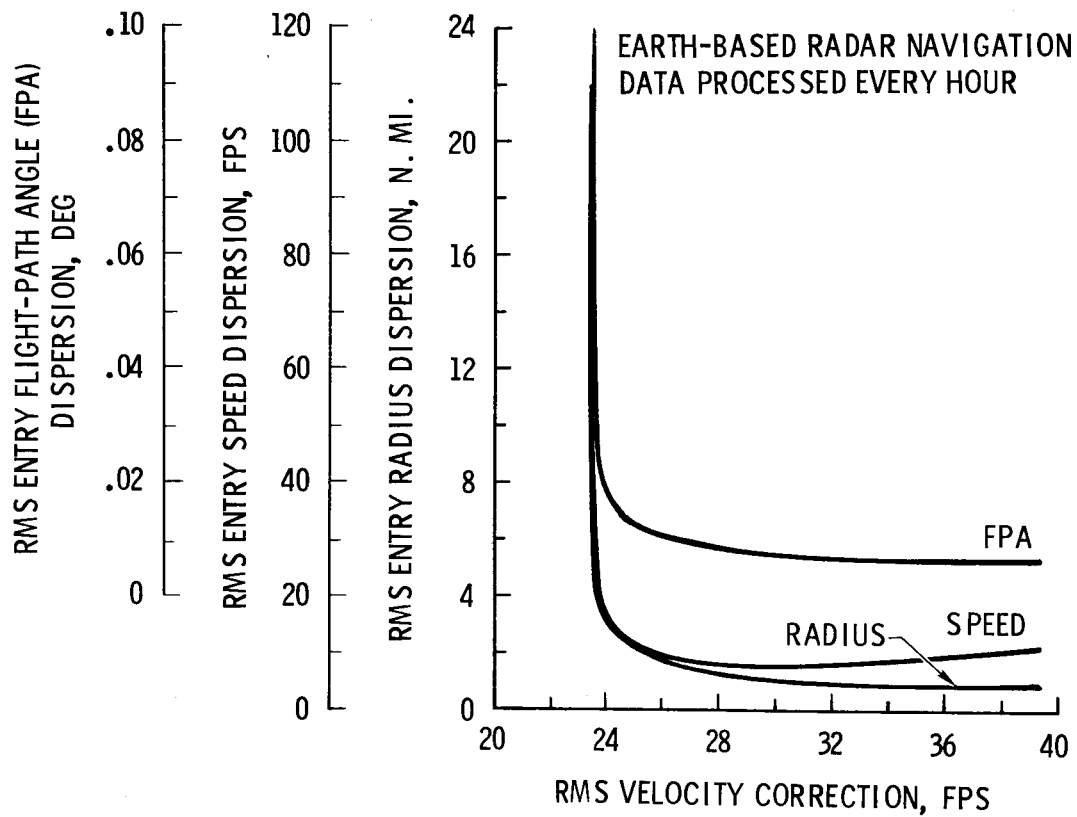
(B) NULL RADIAL, CROSS-RANGE, AND  
FLIGHT-PATH ANGLE (FPA) ERRORS;  
MINIMIZE THE MAGNITUDE OF  
THE COMMANDED CORRECTION.

FIGURE 4.- CONTINUED.



(C) NULL RADIAL, CROSS-RANGE, AND FLIGHT-PATH  
ANGLE (FPA) ERRORS; MINIMIZE THE DISTANCE  
TO THE NOMINAL ENTRY POINT.

FIGURE 4.- CONTINUED.



(D) NULL POSITION VECTOR ERRORS;  
CHOOSE TIME VARIATION SUCH  
THAT FLIGHT-PATH ANGLE (FPA)  
ERRORS ARE ZERO.

FIGURE 4.- CONCLUDED.

## REFERENCES

1. Battin, Richard H.: Astronautical Guidance. McGraw-Hill Book Company, Inc. (New York, N. Y.), 1964.
2. Stern, Robert G.: Interplanetary Midcourse Guidance Analysis. NASA CR-51827, 1963.
3. White, John S.; Callas, George P.; and Cicolani, Luigi S.: Application of Statistical Filter Theory to the Interplanetary Navigation and Guidance Problem. NASA TN D-2697, 1965.
4. Murtagh, Thomas B.; Lowes, Flora B.; and Bond, Victor R.: Navigation and Guidance Analysis of a Mars Probe Launched from a Manned Flyby Spacecraft. NASA TN D-4512, 1968.
5. Robbins, Howard M.: An Analytical Study of the Impulsive Approximation. AIAA Journal, Volume 4, No. 8, pp 1417-1423, August 1966.
6. Cicolani, Luigi S.: Linear Theory of Impulsive Velocity Corrections for Space Mission Guidance. NASA TN D-3365, 1966.
7. Tempelman, Wayne: Linearized Impulsive Guidance Laws. AIAA Journal, Volume 3, No. 11, pp 2148-2149, November 1965.
8. Lowes, Flora B.; and Murtagh, Thomas B.: Navigation and Guidance Systems Performance for Three Typical Manned Interplanetary Missions. NASA TN D-4629, 1968.
9. Murtagh, Thomas B.: Optimum Interplanetary Midcourse Velocity Correction Schedules. Paper to be presented at the IVth Congress of the International Federation of Automatic Control (IFAC) to be held in Warsaw, Poland, June 16-21, 1969.